



Arctic winter 2005: Implications for stratospheric ozone loss and climate change

M. Rex,¹ R. J. Salawitch,² H. Deckelmann,¹ P. von der Gathen,¹ N. R. P. Harris,³ M. P. Chipperfield,⁴ B. Naujokat,⁵ E. Reimer,⁵ M. Allaart,⁶ S. B. Andersen,⁷ R. Bevilacqua,⁸ G. O. Braathen,⁹ H. Claude,¹⁰ J. Davies,¹¹ H. De Backer,¹² H. Dier,¹³ V. Dorokhov,¹⁴ H. Fast,¹¹ M. Gerding,¹⁵ S. Godin-Beekmann,¹⁶ K. Hoppel,⁸ B. Johnson,¹⁷ E. Kyrö,¹⁸ Z. Litynska,¹⁹ D. Moore,²⁰ H. Nakane,²¹ M. C. Parrondo,²² A. D. Risley Jr.,²³ P. Skrivankova,²⁴ R. Stübi,²⁵ P. Viatte,²⁶ V. Yushkov,¹⁴ and C. Zerefos²⁷

Received 27 April 2006; revised 26 May 2006; accepted 12 September 2006; published 8 December 2006.

[1] The Arctic polar vortex exhibited widespread regions of low temperatures during the winter of 2005, resulting in significant ozone depletion by chlorine and bromine species. We show that chemical loss of column ozone (ΔO_3) and the volume of Arctic vortex air cold enough to support the existence of polar stratospheric clouds (V_{PSC}) both exceed levels found for any other Arctic winter during the past 40 years. Cold conditions and ozone loss in the lowermost Arctic stratosphere (e.g., between potential temperatures of 360 to 400 K) were particularly unusual compared to previous years. Measurements indicate $\Delta O_3 = 121 \pm 20$ DU and that ΔO_3 versus V_{PSC} lies along an extension of the compact, near linear relation observed for previous Arctic winters. The maximum value of V_{PSC} during five to ten year intervals exhibits a steady, monotonic increase over the past four decades, indicating that the coldest Arctic winters have become significantly colder, and hence are more conducive to ozone depletion by anthropogenic halogens. **Citation:** Rex, M., et al. (2006), Arctic winter 2005: Implications for stratospheric ozone loss and climate change, *Geophys. Res. Lett.*, 33, L23808, doi:10.1029/2006GL026731.

1. Introduction

[2] Chemical loss of Arctic ozone for particular winters exhibits large variability, driven by variations in tempera-

ture. However, the volume of air cold enough to allow for the existence of polar stratospheric clouds (PSCs) in the Arctic vortex, averaged over winter (V_{PSC}), exhibits a compact, near linear relation with chemical loss of column ozone (ΔO_3) [Rex et al., 2004; Tilmes et al., 2004].

[3] The Arctic winter of 2005 was unusually cold. The geographical extent of temperatures below the PSC formation threshold (A_{PSC}) at particular potential temperature (Θ) levels was high for a broad vertical region of the polar vortex. For Θ of 475 to 500 K, the evolution of A_{PSC} largely followed the previous record values from winter 2000 (see auxiliary material¹). Below 400 K, daily values of A_{PSC} reached record levels for many weeks and the winter average was 50 to 60% larger than previously observed. For 2005, V_{PSC} (vertical integral of A_{PSC}) reached a value 25% larger than the previous record value from winter 2000.

[4] Here, we quantify ΔO_3 using a variety of techniques. The relation between ΔO_3 and V_{PSC} is examined. Finally, a time series for V_{PSC} is shown that indicates the coldest Arctic stratosphere winters, during the past forty years, have become progressively colder.

2. Ozone Loss Estimates for Winter 2005

[5] Different approaches and data sets are used to characterize chemical ozone loss during the Arctic winter 2005.

¹Research Unit Potsdam, Alfred Wegener Institute for Polar and Marine Research, Potsdam, Germany.

²Jet Propulsion Laboratory, California Institute of Technology, Pasadena, California, USA.

³European Ozone Research Coordinating Unit, University of Cambridge, Cambridge, UK.

⁴School of Earth and Environment, University of Leeds, Leeds, UK.

⁵Meteorological Institute, Freie Universität Berlin, Berlin, Germany.

⁶Royal Netherlands Meteorological Institute, De Bilt, Netherlands.

⁷Danish Meteorological Institute, Copenhagen, Denmark.

⁸Naval Research Laboratory, Washington, DC, USA.

⁹Norwegian Institute for Air Research, Kjeller, Norway.

¹⁰Deutscher Wetterdienst, Meteorologisches Observatorium Hohenpeißenberg, German Weather Service, Hohenpeißenberg, Germany.

¹¹Meteorological Service of Canada, Toronto, Ontario, Canada.

¹²Royal Meteorological Institute of Belgium, Brussels, Belgium.

¹³Meteorological Observatory Lindenberg, Lindenberg, Germany.

¹⁴Central Aerological Observatory, Moscow, Russia.

¹⁵Leibniz-Institut für Atmosphärenphysik, Kühlungsborn, Germany.

¹⁶Service d'Aéronomie, CNRS, Institut Pierre-Simon Laplace, Paris, France.

¹⁷Earth System Research Laboratory, NOAA, Boulder, Colorado, USA.

¹⁸Sodankylä Meteorological Observatory, Sodankylä, Finland.

¹⁹Institute of Meteorology and Water Management, Centre of Aerology, Legionowo, Poland.

²⁰Met Office, Exeter, UK.

²¹Asian Environmental Research Group, National Institute for Environmental Studies, Tsukuba, Japan.

²²Instituto Nacional de Tecnica Aeroespacial, Madrid, Spain.

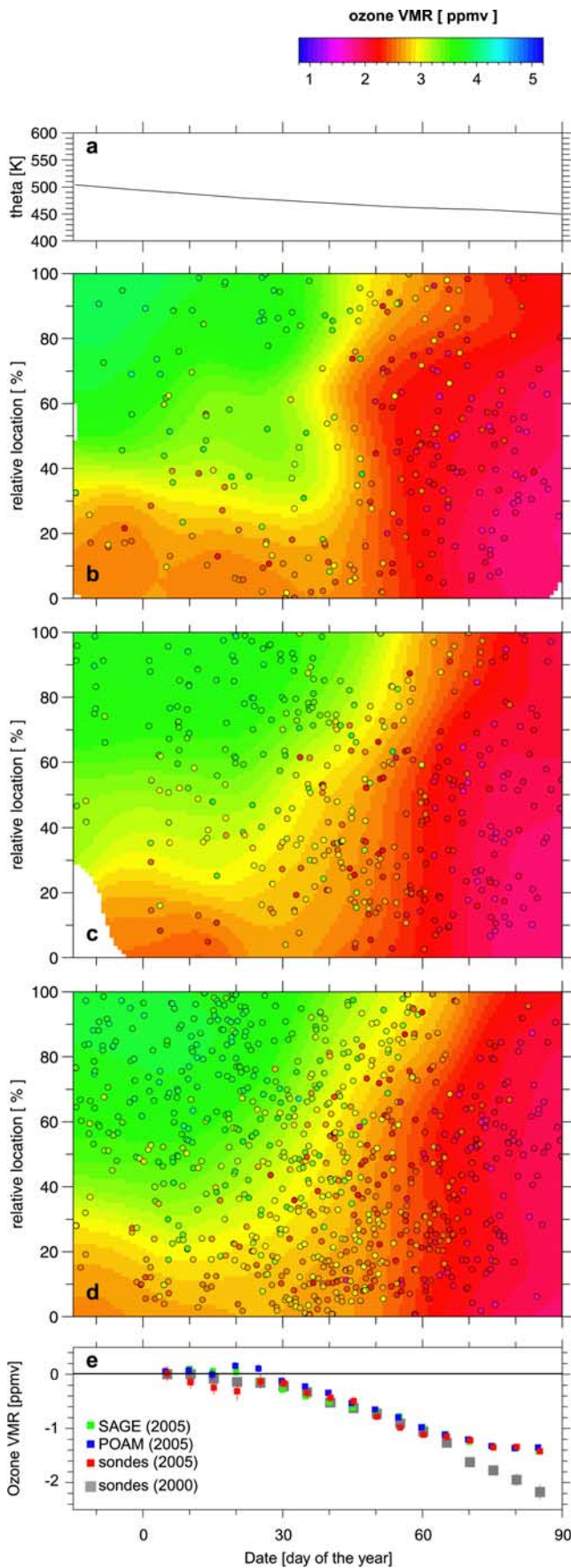
²³Science Applications International Corporation, Hampton, Virginia, USA.

²⁴Czech Hydrometeorological Institute, Prague, Czech Republic.

²⁵Swiss Meteorological Aerological Station, Payerne, Switzerland.

²⁶Federal Office of Meteorology and Climatology, MeteoSwiss, Payerne, Switzerland.

²⁷Laboratory of Climatology and Atmospheric Environment, University of Athens, Greece.



We consider estimates based on regression analysis of data from the northern hemisphere ozone sonde station network (hereafter, ozonesondes) for air parcels sampled at different times (March) [e.g., *Rex et al.*, 1999] and estimates based on the “vortex average descent” approach, applied to measurements by the SAGE III [*Randall et al.*, 2005] and POAM III [*Hoppel et al.*, 2002] satellite instruments. First, we describe the morphology of ozone near 450 K, which was notably different than for other cold Arctic winters.

2.1. Ozone Distribution and Evolution

[6] Figure 1 shows the evolution of ozone inside the Arctic polar vortex (defined by the region enclosed by the maximum gradient in potential vorticity versus equivalent latitude) on the 450 K equivalent potential temperature ($e\Theta$) surface, from mid-December 2004 to March 2005, as observed by sondes, SAGE III, and POAM III. The quantity $e\Theta$ represents the value of Θ an air mass would achieve on 31 March using calculated, vortex average descent rates [*Rex et al.*, 2004]. The top plot shows the time evolution of Θ for the $e\Theta = 450$ K surface. In the absence of chemical loss and mixing, O_3 should be conserved on an $e\Theta$ surface. Figure 1e shows the evolution of vortex averaged ozone on the $e\Theta = 450$ K surface for the winter of 2005 from sondes, SAGE III and POAM III, compared to the same quantity as observed by sondes for the winter of 2000 [from *Rex et al.*, 2002]. The data show a steady decline of ozone within the vortex between late January and early March. About 1.5 ppmv ozone was lost during the winter.

[7] The initial ozone field inside the polar vortex was characterized by relatively low ozone mixing ratios in the core of the vortex (inner 30% of the vortex area). Due to this horizontal gradient, inhomogeneities in sampling can result in uncertainties of ozone loss estimates from the vortex average [*Hoppel et al.*, 2002] or the tracer relation [*Tilmes et al.*, 2004] approaches. The sampling of the vortex by the three instruments used in this study is shown in Figures 1b–1d. Overall the sampling was quite homogenous for all instruments, with the exception of a ten day period in late January, when the sampling from the sondes was biased towards the core of the vortex (Figure 1b). A temporary dip in vortex averaged ozone from the sondes occurs at this time but has no impact on our overall ozone loss estimates. The fact that ozone loss estimates from all these instruments

Figure 1. (a) Time evolution of Θ on the $e\Theta = 450$ K surface. Measured ozone inside the Arctic vortex as a function of time and location relative to the vortex core, for the $e\Theta = 450$ K surface, from (b) sondes, (c) SAGE III, and (d) POAM III. Circles indicate time, location and O_3 of actual measurements. Location relative to the vortex core (relative location = 0%) and vortex edge (relative location = 100%) found using equivalent latitude, allowing for daily variations in vortex size [see *Rex et al.*, 1999]. Contour shading calculated by averaging over the closest measurements, gaussian weighted by distance in date/relative location space. (e) Time evolution of vortex averaged ozone mixing ratio on the $e\Theta = 450$ K surface, from sondes, SAGE III, and POAM III (as indicated) for 2005 and from sondes for the Arctic winter of 2000.

380-550K partial column loss estimates:

winter of 2004/2005

- Match: 127 +/- 21 DU
- sondes: 121 DU
- SAGE: 110 DU
- POAM: 113 DU

winter of 1999/2000:

- sondes: 96 DU

winter of 1995/1996

- sondes: 105 DU (not shown)

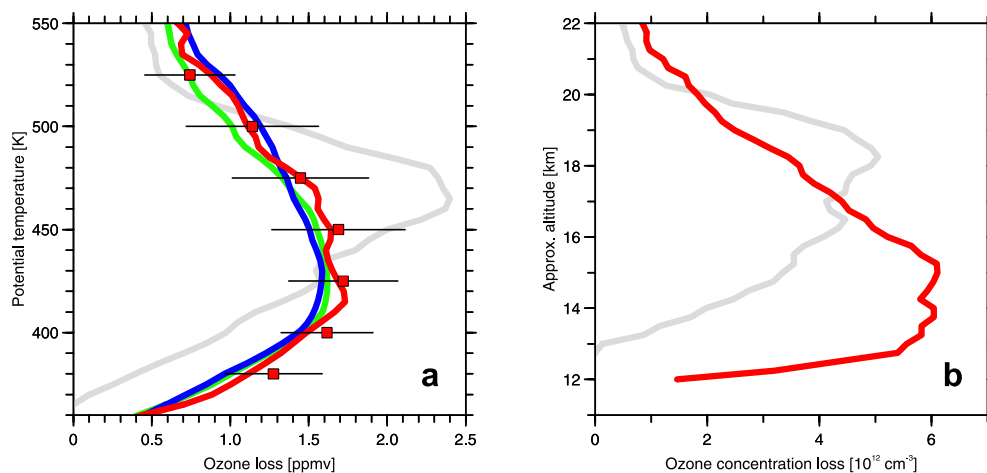


Figure 2. (a) Accumulated ozone loss mixing ratio (ppmv) between 5 Jan and 25 March, versus $e\Theta$, from the vortex averaged sonde method for the winters of 2005 and 2000. Also shown are ozone losses from Match and from the time evolution of vortex averaged ozone from SAGE III and POAM III. Error bars from Match represent 1σ statistical uncertainties; additional systematic uncertainties are in the order of 20%. (b) Same as Figure 2a, except ozone loss concentration is shown from the vortex averaged sonde method for 2005 and 2000. Tabulation of chemical loss of column ozone by the various methods is also given.

agree well (Figure 1e) increases our confidence that sampling issues do not have a significant impact on our results.

2.2. Ozone Loss Profiles

[8] Figure 2a compares the vertical profile of ozone loss at the end of the winter derived from Match with results from the vortex average approach. We find a broad vertical range of ozone loss around 1.5 ppmv between Θ of 400 and 450 K. Good agreement is found at all Θ levels, further increasing our confidence that sampling or mixing issues have not influenced our results. With Match we can separate ozone changes during dark sections along the air mass trajectories from changes that occurred during sunlit portions of the trajectories [Rex *et al.*, 1999]. Figure S2 of the auxiliary material shows that changes in ozone during dark portions of the trajectories are small and if anything positive, suggesting dynamical effects did not significantly impact our estimates of ozone loss and would only lead to an underestimation of the loss rates.

[9] Figure 2a also shows the ozone loss profile for the winter of 2000 found using the vortex averaged descent approach. The maximum ozone loss for the 2005 winter, in terms of mixing ratios, was smaller than the record value reached in a narrow vertical region for the winter of 2000. This is consistent with the finding of Manney *et al.* [2006].

2.3. Total Column Loss

[10] The quantity most relevant for the biosphere is total ozone column. Losses of total column ozone are driven by the vertical distribution of the change in ozone concentration, shown in Figure 2b. The loss of total column ozone that occurred from 5 January to 25 March 2005, between $e\Theta$ levels of 380 and 550 K, was 121 DU. This quantity is based on the vertical integral of the vortex averaged sonde data points in Figure 2b; the uncertainty of this estimate is ~ 20 DU. Similar ozone loss is found by other instruments and from Match (Figure 2). Compared to winter 2000, the ozone loss profile in 2005 extended to lower altitudes, where ozone concentrations are large. Loss of column

ozone for the winter of 2005 exceeds those measured during the winters of 1996 (105 DU) and 2000 (96 DU), which are the largest losses recorded previously (all values for $e\Theta$ between 380 and 500 K). Hence, the winter of 2005 had a larger chemical loss of column ozone than any other winter during the past 40 years, although the uncertainty of the loss for this winter overlaps with the uncertainty of the loss for two previous cold winters.

[11] Quantifications of ozone losses in the vertical region below 400 K are sensitive to mixing issues (exchange of air across the edge of the polar vortex) and uncertainties in the calculated diabatic subsidence rates. The good agreement between results from Match and from the vortex average approach at 380 K (Figure 2a) suggests that mixing did not have a major impact on our ozone loss estimates at these levels. Also, we have not diagnosed substantial ozone losses in this vertical region for most previous winters (and for none of the warm winters), suggesting that the approach does not tend to produce artifacts. The larger ozone losses observed at these levels for winter 2005 are consistent with the fact that low temperatures extended to lower altitudes in this winter, compared to the previous cold winters. Note that ozone loss estimates near the bottom of the vortex are generally less reliable [e.g., Knudsen *et al.*, 1998]. Hence, the uncertainties of the loss estimates for the region below 400K are generally larger than those for the region above. But our overall conclusions still hold if the analysis is restricted to Θ levels above 400 K (auxiliary material¹).

3. Arctic Ozone Loss and Climate Change

[12] Based on data from the vortex average approach, Rex *et al.* [2004] reported a compact relationship between ΔO_3 and V_{PSC} . This relation was confirmed by an analysis of HALOE data using the tracer relation approach [Tilmes *et*

¹Auxiliary material data sets are available at <ftp://ftp.agu.org/apend/gl/2006gl026731>. Other auxiliary material files are in the HTML.

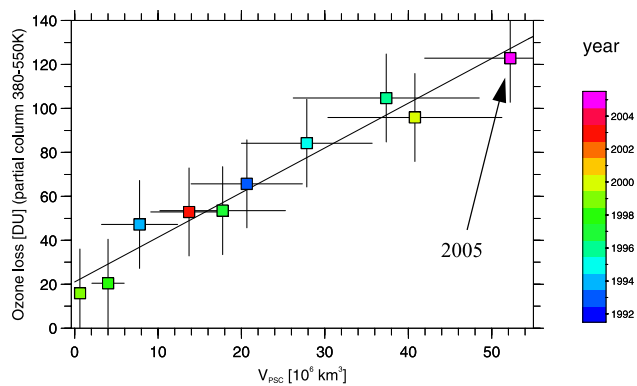


Figure 3. ΔO_3 versus V_{PSC} for Arctic winters between 1993 and 2005 (no values for the warm winters of 2001, 2002, 2004 due to major mid-winter warmings and/or lack of sufficient ozone sonde measurements). Value for 2005 is indicated. Values for other winters from Rex *et al.* [2004], except all values are calculated between $e\Theta$ levels of 380 and 550 K. V_{PSC} is found using temperatures from ECMWF, $H_2O = 5$ ppmv, and an observed profile of HNO_3 [Rex *et al.*, 2002]. The Figure is very similar if FU-Berlin data is used up to 2002 (no FU-Berlin data available after 2002). Error bars for ΔO_3 represent an upper limit of 20 DU uncertainty and for V_{PSC} uncertainty due to 1 K uncertainty in temperature. The line indicates a linear least squares fit to the points and has a slope of 15.6 DU/K cooling, based on 7.7×10^6 km³ additional V_{PSC} per Kelvin uniform cooling [Rex *et al.*, 2004]. The correlation coefficient is 0.98 with a statistical significance larger than 99.9% and an uncertainty of +0.02/−0.14 (the autocorrelation of both time series was considered for the estimation of the significance by reducing the degrees of freedom according to standard statistics; a Monte-Carlo approach was used to estimate the uncertainty: 99.9% of correlation coefficients exceed 0.84, calculated for 1000 data sets with random noise added to ΔO_3 and V_{PSC} , corresponding to the uncertainty of the individual points).

al., 2004]. The observations of ΔO_3 and V_{PSC} for the winter 2005 lie along an extension of the near linear relation between these quantities observed for prior winters (Figure 3).

[13] Figure 4 shows the evolution of V_{PSC} over the past four decades. The unusually cold Arctic winter 2005 extends the long term upward trend of maximum values of V_{PSC} over the past ~forty years described by Rex *et al.* [2004]. A linear fit through the solid points in Figure 4, which represent maximum values of V_{PSC} for 5 year intervals, has a slope of $9.9 \pm 1.1 \times 10^6$ km³ per decade, similar to the slope given by Rex *et al.* [2004]. The conclusion of a large, steady rise in the maximum value of V_{PSC} does not depend on the length of the time interval or the end points chosen for the analysis (auxiliary material). The strong relation between ΔO_3 and V_{PSC} indicates V_{PSC} is the relevant parameter for relating changes in stratospheric temperature to ozone loss. Indeed, the notion of “coldest Arctic winters getting colder” can be overlooked in analyses of temperature trends [e.g., Manney *et al.*, 2005].

[14] It is unclear why the Arctic vortex has recently exhibited severely cold winters. To explore the robustness

of the observed trend, we have generated 10^6 random permutations of the V_{PSC} data set in a Monte-Carlo simulation, ensuring that the random data sets have the same probability density function as the original data. Table 1 gives the probabilities to observe a trend equal to or larger than the observed trend of the cold winters (prob1). A second entry, prob2, is based on the same Monte-Carlo simulations. It gives the probability of observing a trend equal to or larger than the observed trend, with the additional constraint that the uncertainty of the slope is equal to or smaller than the uncertainty of the observed trend. The trend estimates and probabilities are given for 5 and 10 year intervals for the selection of the maximum values of V_{PSC} (details for all intervals between 4 and 10 years are in the auxiliary material). The calculation is repeated assuming: (a) a 1K warm bias of the old radiosonde data (second column); (b) use of the FU-Berlin data alone up to 2002 (again assuming a 1K warm bias for the early data) and V_{PSC} from ECMWF for the remaining years reduced by the maximum difference between the FU-Berlin data and the ECMWF data during the 22-year overlap period (third column); (c) as (b) but adding random noise corresponding to an additional 1K 2σ statistical uncertainty of the temperature data, before calculating the trend (fourth column). Table 1 shows it is very unlikely (well below 1% probability) that the observed trend toward colder winters is a purely random event or is caused by inconsistencies in the meteorological data sets.

[15] Chemistry climate models (CCMs) provide insight into processes controlling the temperature of the Arctic vortex, but results from various studies are contradictory. Shindell *et al.* [1998] suggested decreases in planetary wave activity reaching the mid-latitude stratosphere due to increased westerly winds in the subtropics would lead to stronger, colder Arctic vortices due to climate change associated with rising greenhouse gases (GHGs). Schnadt *et al.* [2002], however, showed a CCM coupled to an oceanic model resulted in a tendency for future warmer, less stable Arctic vortices, a consequence of increased

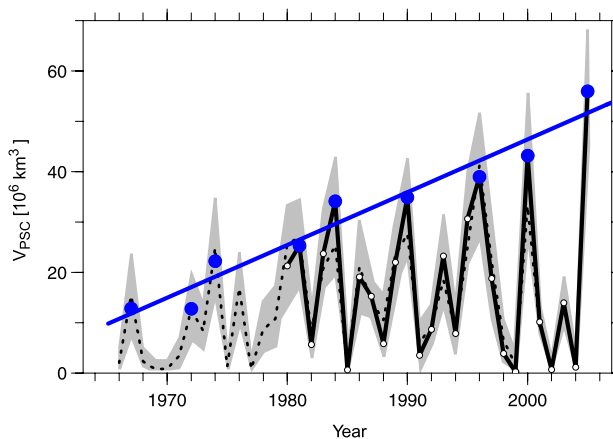


Figure 4. V_{PSC} over the past 40 years from ECMWF data (solid line) and FU-Berlin data (dashed line). See Rex *et al.* [2004] for a discussion of the FU-Berlin data. V_{PSC} has been calculated between 380 and 550 K for all years. The gray shading represents uncertainty of V_{PSC} due to 1 K uncertainty of the long term stability of radiosonde temperatures.

Table 1. Trend Estimates and Probability for Occurrence of Estimated Trend in Random Data

	Original	1K Radiosonde Trend (Assuming Warm Bias for Old Sondes ^a)	1K Radiosonde Trend + ECMWF Data Reduced	1K Radiosonde Trend + 1K Statistical Uncertainty + ECMWF Data Reduced
		<i>Interval 5 years</i>		
Original trend, 10 ⁶ km ³ /year	0.99 ± 0.11	0.80 ± 0.13	0.60 ± 0.15	0.60 ± 0.15
prob1/prob2, %	0.04/<0.0001	0.4/0.002	0.8/0.03	0.9/0.04
		<i>Interval 10 years</i>		
Original trend, 10 ⁶ km ³ /year	1.03 ± 0.14	0.73 ± 0.14	0.59 ± 0.21	0.59 ± 0.21
prob1/prob2, %	0.04/0.004	0.4/0.03	0.5/0.3	0.7/0.3

^aSee text.

planetary wave activity associated with rising sea surface temperatures, contradicting earlier CCM calculations that suggested a tendency to future colder, more stable Arctic vortices [Austin et al., 1992].

[16] The increased variability of Arctic stratospheric temperature conditions during recent years [Manney et al., 2005] could indicate that the mechanism described by Shindell et al. [1998] acts efficiently during periods of relatively weak dynamic activity, hence during stratospheric conditions that are closer to radiative equilibrium. According to this mechanism, increasing GHGs lead to a stronger meridional temperature gradient during such periods and vertically propagating waves are deflected more equatorwards, leading to further cooling at high latitudes for such situations. On the other hand, an overall increase in momentum flux from the troposphere [Schnadt et al., 2002] could make these conditions less frequent. While quite speculative, this combination of behaviors could be the cause of relatively few cold winters in recent years, but an increase in the severity of the winters that are cold.

[17] We lack a fundamental understanding of the factors responsible for the rise in maximum value of Arctic V_{PSC} shown in Figure 4. Nonetheless, the extension of this time series to a new record value for V_{PSC} in the winter of 2005 is cause for concern. If climate forcing from increasing GHGs plays a role in rising maximum V_{PSC}, the tendency toward colder Arctic winters will likely continue. In this case, Arctic ozone loss could continue to get worse until around the year 2020, when declining levels of anthropogenic halogens will eventually reduce chemical loss [Knudsen et al., 2004]. A reliable assessment of future levels of Arctic ozone will not be possible until the observed tendency toward colder Arctic winters is understood.

[18] **Acknowledgments.** Meteorological data were provided by ECMWF and FU-Berlin. This work was supported by the BMBF (DYCHO, FKZ07ATC08) and by the EC (project SCOUT-O3). Ozone-sondes were partially funded by the EC (project QUOBI). Research at the Jet Propulsion Laboratory, California Institute of Technology, is performed under contract with the National Aeronautics and Space Administration. We thank T. Nagai and C. Trepte for providing ozone data for this study and E. Weatherhead for helpful discussions.

References

Austin, J., N. Butchart, and K. P. Shine (1992), Possibility of an Arctic ozone hole in a doubled CO₂ climate, *Nature*, *360*, 221–225.
 Hoppel, K., R. Bevilacqua, G. Nedoluha, C. Deniel, F. Lefèvre, J. Lumpe, M. Fromm, C. Randall, J. Rosenfield, and M. Rex (2002), POAM III observations of arctic ozone loss for the 1999/2000 winter, *J. Geophys. Res.*, *107*(D20), 8262, doi:10.1029/2001JD000476.
 Knudsen, B. M., et al. (1998), Ozone depletion in and below the Arctic vortex for 1997, *Geophys. Res. Lett.*, *25*, 627–630.

Knudsen, B. M., et al. (2004), Extrapolating future Arctic ozone losses, *Atmos. Chem. Phys.*, *4*, 1849–1856.
 Manney, G. L., K. Krüger, J. L. Sabutis, S. A. Sena, and S. Pawson (2005), The remarkable 2003–2004 winter and other recent warm winters in the Arctic stratosphere since the late 1990s, *J. Geophys. Res.*, *110*, D04107, doi:10.1029/2004JD005367.
 Manney, G. L., M. L. Santee, L. Froidevaux, K. Hoppel, N. J. Livesey, and J. W. Waters (2006), EOS MLS observations of ozone loss in the 2004–2005 Arctic winter, *Geophys. Res. Lett.*, *33*, L04802, doi:10.1029/2005GL024494.
 Randall, C. E., et al. (2005), Reconstruction and simulation of stratospheric ozone distributions during the 2002 austral winter, *J. Atmos. Sci.*, *62*, 748–764.
 Rex, M., et al. (1999), Chemical ozone loss in the Arctic winter 1994/95 as determined by the Match technique, *J. Atmos. Chem.*, *32*, 35–59.
 Rex, M., et al. (2002), Chemical depletion of Arctic ozone in winter 1999/2000, *J. Geophys. Res.*, *107*(D20), 8276, doi:10.1029/2001JD000533.
 Rex, M., R. J. Salawitch, P. von der Gathen, N. R. P. Harris, M. P. Chipperfield, and B. Naujokat (2004), Arctic ozone loss and climate change, *Geophys. Res. Lett.*, *31*, L04116, doi:10.1029/2003GL018844.
 Schnadt, C., et al. (2002), Interaction of atmospheric chemistry and climate and its impact on stratospheric ozone, *Clim. Dyn.*, *18*, 501–517.
 Shindell, D. T., D. Rind, and P. Lonergan (1998), Increased polar stratospheric ozone losses and delayed eventual recovery owing to increasing greenhouse-gas concentrations, *Nature*, *392*, 589–592.
 Tilmes, S., et al. (2004), Ozone loss and chlorine activation in the Arctic winters 1991–2003 derived with the tracer-tracer correlations, *Atmos. Chem. Phys.*, *4*, 2181–2213.

M. Allaart, KNMI, Postbus 201, NL-3730 AE, De Bilt, Netherlands.
 S. B. Andersen, Danish Meteorological Institute, Lyngbyvej 100, DK-20100 Copenhagen, Denmark.
 R. Bevilacqua and K. Hoppel, Naval Research Laboratory, Code 7227, Washington, DC 20375-5320, USA.
 G. O. Braathen, NILU, N-2027 Kjeller, Norway.
 M. P. Chipperfield, School of Earth and Environment, University of Leeds, Leeds LS2 9JT, UK.
 H. Claude, Met. Obs. Hohenpeißenberg, German Weather Service, Albin-Schwaiger-Weg 10, D-82383 Hohenpeißenberg, Germany.
 J. Davies and H. Fast, Met. Service of Canada, 4905 Dufferin Street, Toronto, ON, Canada M3H 5T4.
 H. De Backer, Royal Meteorological Institute of Belgium, B01180 Brussels, Belgium.
 H. Deckelmann, M. Rex, and P. von der Gathen, Research Unit Potsdam, Alfred Wegener Institute for Polar and Marine Research, P.O. Box 600149, D-14401 Potsdam, Germany. (mrex@awi-potsdam.de)
 H. Dier, MOL, Am Observatorium 12, D-15848 Tauche/OT Lindenberg, Germany.
 V. Dorokhov and V. Yushkov, CAO, Dolgoprudny, Moscow, Russia.
 M. Gerding, IAP, D-18225 Kühlungsborn, Germany.
 S. Godin-Beekmann, Service d'Aéronomie, CNRS, Institut Pierre-Simon Laplace, UPMC-b102, 4 Place Jussieu, P-75252 Paris Cedex 05, France.
 N. R. P. Harris, European Ozone Research Coordinating Unit, University of Cambridge, Cambridge CB2 1EW, UK.
 B. Johnson, Earth System Research Laboratory, NOAA, 325 Broadway, Boulder, CO 80305, USA.
 E. Kyrö, SMO, Sodankylä, Finland.
 Z. Litynska, MWM, Centre of Aerology, Zegrzynska 39, PL-05119 Legionowo, Poland.
 D. Moore, Met Office, FitzRoy Road, Exeter EX1 3PB, UK.
 H. Nakane, Asian Environmental Research Group, NIES, 16-2, Onogawa, Tsukuba, Ibaraki 305-8506, Japan.

B. Naujokat and E. Reimer, Met. Institute, Freie Universität Berlin, C.-H.-Becker-Weg 6-10, D-12165 Berlin, Germany.

M. C. Parrondo, INTA, Crta de Ajalvir km 4, E-28850 Torrejon de Ardoz, Madrid, Spain.

A. D. Risley Jr., SAIC, One Enterprise Parkway, Suite 270, Hampton, VA 23666, USA.

R. J. Salawitch, Jet Propulsion Laboratory, California Institute of Technology, Pasadena, CA 91109, USA.

P. Skrivankova, Czech Hydrometeorological Institute, Na Sabatce 17, 143 06 Praha 4, Czech Republic.

R. Stübi, Swiss Meteorological Aerological Station, CH-1530 Payerne, Switzerland.

P. Viatte, Federal Office of Meteorology and Climatology, MeteoSwiss, CH-1530 Payerne, Switzerland.

C. Zerefos, Laboratory of Climatology and Atmospheric Environment, University of Athens, GR-15784 Athens, Greece.

1 **Auxiliary Material for Rex et al., Arctic winter 2005: Implications for stratospheric**
2 **ozone loss and climate change, Manuscript 2006GLxxxxxx**

3 The main body of the paper states “changes in ozone during the dark portions of the
4 trajectories are very small, which also suggest that dynamical effects (e.g. mixing,
5 uncertainties in calculated subsidence rates, systematic drift of trajectories in equivalent
6 latitude space) did not significantly impact our results”. Figure 3a illustrates a profile of
7 the accumulated ozone loss from Match for the Arctic winter of 2004-05. These values
8 are found by quantifying changes in ozone for air masses sampled at different times along
9 calculated Lagrangian trajectories [Rex et al., 1999]. The analysis accounts for diabatic
10 descent and avoids trajectories that were likely influenced by mixing.

11

12 The Match technique allows for calculation of changes in ozone along the sunlit and dark
13 portions of the Lagrangian trajectories [Rex et al., 1999]. Figure 5 shows profiles of
14 ozone loss rates for the sunlit and dark portions of the trajectories. The ozone change
15 during night-time is positive, but close to zero. Since chemical loss of ozone is expected
16 to cease during dark periods, the deviation of the night-time points from zero serves as a
17 reasonable estimate of the uncertainty in the Match-based losses to effects of irreversible
18 mixing, uncertainties in subsidence rates, and errors in the trajectories. Much larger loss
19 is found for the day-time portion in the trajectories, indicating the above noted
20 uncertainties do not have a large affect on the estimates of ΔO_3 found in this study. The
21 ozone loss estimates reported in the paper could perhaps slightly underestimate the actual
22 loss, since the changes observed during darkness all tend to be positive.

23

1 Values of ΔO_3 given in this study are found by integrating accumulated chemical loss
2 between the 380 and 550 K equivalent spring potential temperature surfaces. In *Rex et al.*
3 [2004], chemical loss was found by integrating between the 400 and 550 K surfaces. The
4 present analysis has been extended to lower potential temperature levels, for the Arctic
5 winter of 2005, because temperatures below 400 K were lower than had been observed
6 for any other winter since 1991. As a result, below 400 K, A_{PSC} averaged over winter was
7 significantly higher in 2005 than for the Arctic winter of 2000. The unusually cold
8 conditions at lower potential temperature levels for the winter of 2005 is further
9 illustrated in Figure 6, which shows the time evolution, at 4 potential temperature levels,
10 of daily values of A_{PSC} for the 2000 and 2005 winters as well as the range of variability
11 since 1992. Meteorological conditions for the most recent Arctic winter require extending
12 the definition of ΔO_3 and V_{PSC} to lower altitudes, in order to capture the full extent of
13 chemical loss of column ozone. Since the uncertainties of ozone loss estimates increase
14 for lower altitudes (as discussed in the main text), a compromise of a lower limit of 380
15 K limit has been chosen for this analysis presented in the main body of the paper.

16

17 Figure 7 shows a plot of ΔO_3 versus V_{PSC} , for values between 400 and 550 K (as has been
18 previously used in our prior publications) and using 360 K as the lower limit of
19 integration. While only using a low limit of 360K includes the full vertical range where
20 ozone loss occurred, it also largely increases the uncertainties of the estimates. In some
21 years the vortex has not extended down to this level and the values for the vertical range
22 360-500K given here have large uncertainties. Therefore a compromise of 380K is used
23 in the main body of the paper. The relations for all three vertical ranges are similar, and

1 winter 2005 exhibits larger values of ΔO_3 and V_{PSC} than observed during previous
2 winters, for all three integration limits. Hence, as stated in the main paper, our overall
3 conclusions still hold if the analysis is restricted to θ levels above 400K.

4

5 *Manney et al.* [2006], who state “despite record cold, chemical O_3 loss was less in 2005
6 than in previous cold winters”, restrict their analysis of MLS data to potential temperature
7 levels above 400 K. Also, their analysis is based on chemical loss of ozone mixing ratio,
8 rather than chemical loss of ozone concentration, and their ozone loss calculation
9 extended only to early March. Figure 6 of *Manney et al.* [2006], which shows ozone loss
10 (ppmv) versus Θ extending to 350 K from POAM III, clearly shows that greater loss
11 occurred below 400 K for the winter of 2005 than in previous winters. An estimate of the
12 chemical loss of column ozone using the data in Figure 6 of *Manney et al.* [2006] would
13 likely result in the conclusion that loss during the winter of 2005 exceed the amount of
14 loss found for any previous cold winter.

15

16 In the main body of the paper, we state that the observed trend of maximum V_{PSC} versus
17 time does not depend on the choice of time interval chosen to select the maximum values.

18 To explore whether the observed trend in the maximum values of V_{PSC} depends on the
19 time interval, we have repeated the trend calculations for intervals between 4 and 10
20 years. Table 2 (first column) shows that the calculated trend is largely independent from
21 the choice of the interval.

22

1 In the main body of the paper, we also state that the observed trend of maximum V_{PSC}
2 does not depend on the end points. We have split the overall 40-year period into two 20-
3 year sections, i.e. 1966-1985 and 1986-2005. Table 3 gives the trend estimates for both
4 periods. The individual 20-year trends are similar to the overall trend, are both
5 statistically significant (the values prob1 and prob2 given in the table are explained
6 below) and even somewhat larger than the overall 40-year trend. Only for the 4 year
7 intervals the choice of one particular end point (2004) would lead to a significantly
8 smaller trend estimate, because in this case the last 4-year interval only covers the series
9 of relatively warm winters 2001-2004. But even for this particular sampling the
10 calculated trend is significant to the 97% level. For intervals of 5-10 years the calculated
11 trend is largely independent of the choice of the end-point.

12

13 The paper also presents an estimate of the statistical robustness of the observed trend of
14 maximum V_{PSC} . Further details are given here. To estimate the probability for a trend like
15 the one reported in the main paper to occur in a random data set, we have repeated the
16 analysis with 10^6 random data sets. To ensure that the probability density function of
17 these random data sets is identical to that of the V_{PSC} time series, we have generated these
18 as random permutations of the original V_{PSC} data. Table 2 (first column) shows the
19 results. The probability for a trend equal or larger than the observed trend is given as
20 prob1. The probability that the observed trend is equal or larger, as well as its uncertainty
21 being equal or smaller to that of the observed trend, is given as prob2. All of these
22 probabilities are very small ($< 1.3\%$ for prob1 and $< 0.05\%$ for prob2, with the majority

1 of the cases having much smaller probabilities), indicating it is very unlikely that the
2 observed trend is a random event.

3

4 The long term meteorological data used here relies on the FU-Berlin analysis of
5 radiosondes. Hence, the data set is independent from issues related to changes between
6 the satellite area and the period before or changes in assimilation systems (e.g. *Manney et*
7 *al.*, 2003). But instrumental changes of the radiosondes can introduce a bias. *Lanzante*
8 *and Klein* (2003) showed that 1 K is an upper limit for the impact of these changes on the
9 temperature data. Based on this upper limit, we have repeated the analysis with a
10 modified data set, for which we decreased the old radiosonde temperatures using a linear
11 function equal to 1 K at the start of the time series and zero at the end of the end (second
12 column of Table 2). These calculations result in a modest ~25% reduction in the slope of
13 the maximum V_{PSC} , and in maximum values for prob1 and prob2 of 4 and 0.2%,
14 respectively. Hence, even with an assumption of a 1 K drift of the radiosondes towards
15 colder temperature, we find that the observed trend in V_{PSC} is unlikely to be a random
16 event.

17

18 The third column of Table 2 addresses the possible complications from the use of both
19 FU-Berlin and ECMWF data in the time series for V_{PSC} . The FU-Berlin data ends in 2002
20 and a combination of ECMWF data with FU-Berlin data is used to cover the whole time
21 period. The two data sets overlap by 22 years and agree very well during the overlap
22 (Figure 4). For the third column of Table 2, we have decreased the V_{PSC} data from
23 ECMWF by the maximum difference that occurred during the overlapping period. We

1 have also applied the 1K temperature increase to the old radiosonde data, as described
2 above. Even for this extreme assumption, the slope of the maximum V_{PSC} is about 60% of
3 its original value. The probabilities for the trend to be random are still below 4% and 1%
4 for prob1 and prob2, respectively. Again, this calculation shows that the observed trend
5 towards colder Arctic winters is robust and most likely not random.

6

7 For the final test, represented in column 4 of Table 2, random noise corresponding to an
8 additional statistical 2σ uncertainty of the temperature fields (on top of the 1K systematic
9 trend) was added to the data, before calculating the trend lines. The probabilities for the
10 trend to be random remain below 4% and 1% for prob1 and prob2.

11

12 **References for auxiliary material**

13

14 Lanzante, J.R., S.A. Klein, and D. J. Seidel (2003), Temporal Homogenization of
15 Monthly Radiosonde Temperature Data. Part II: Trends, Sensitivities, and MSU
16 Comparison, *Journal of Climate*, 16, 241-262.

17

18 Manney et al. (2003), Lower stratospheric temperature differences between
19 meteorological analyses in two cold Arctic winters and their impact on polar processing
20 studies, *J. Geophys. Res.*, 108 (D5), 8328, doi: 10.10029/2001JD001149.

21

22 Manney, G. L. *et al.* (2006), EOS MLS observations of ozone loss in the 2004–2005
23 Arctic winter, *Geophys. Res. Lett.*, 33, L04802, doi:10.1029/2005GL024494.

1

2 Rex, M. *et al.* (1999), Chemical Ozone Loss in the Arctic Winter 1994/95 as Determined
3 by the Match Technique, *J. Atmos. Chem.*, 32, 35-59.

4

5 Rex, M. *et al.* (2004), Arctic ozone loss and climate change, *Geophys. Res. Lett.*, 31,
6 L04116, doi:10.1029/2003GL018844.

7

8 **Figure 5.** Ozone loss rate (ppbv/hr) between 5 Jan and 10 Feb 2005 versus Θ , where
9 ozone loss rates are calculated separately for the sunlit and for the dark portions of the
10 trajectories. Error bars denote 1σ statistical uncertainties.

11

12 **Figure 6.** Time series of A_{PSC} for December to March of winter 2000 (blue) and 2005
13 (red) at the $\Theta = 380, 400, 475$ and 550 K levels. Gray shading indicates the range of A_{PSC}
14 between 1992 and 2004 (excluding the winter of 2000). Here, A_{PSC} denotes the *daily*
15 horizontal extent of temperatures low enough for PSCs to exist (in the main paper, we use
16 A_{PSC} to refer to the average value of this quantity over winter).

17

18 **Figure 7.** ΔO_3 versus V_{PSC} for various Arctic winters calculated for $e\theta$ between 400 and
19 550 K (circles, dashed fit line) and for $e\theta$ between 360 and 550 K (boxes, solid fit line).
20 The 400 to 550 K points, for winters prior to 2005, are from *Rex et al.* [2004].

Table 2: Trend estimates and probability for occurrence of estimated trend in random data

Interval	original	1K radiosonde trend (assuming warm bias for old sondes, see text)	1K radiosonde trend and ECMWF data reduced	1K radiosonde trend + 1K statistical Temp. uncertainty, ECMWF data reduced
	Trend [$10^6\text{km}^3/\text{year}$] prob1 / prob2 [%]	Trend [$10^6\text{km}^3/\text{year}$] prob1 / prob2 [%]	Trend [$10^6\text{km}^3/\text{year}$] prob1 / prob2 [%]	Trend [$10^6\text{km}^3/\text{year}$] prob1 / prob2 [%]
4	1.04 ± 0.17 0.01 / 0.0008	0.88 ± 0.20 0.13 / 0.02	0.68 ± 0.20 0.3 / 0.1	0.68 ± 0.20 0.4 / 0.1
5	0.99 ± 0.11 0.04 / <0.0001	0.80 ± 0.13 0.4 / 0.002	0.60 ± 0.15 0.8 / 0.03	0.60 ± 0.15 0.9 / 0.04
6	0.98 ± 0.13 0.7 / 0.02	0.75 ± 0.13 3 / 0.05	0.60 ± 0.16 4 / 0.3	0.60 ± 0.16 4 / 0.3
7	0.97 ± 0.14 1.3 / 0.05	0.73 ± 0.14 4 / 0.1	0.60 ± 0.17 4 / 0.6	0.60 ± 0.17 4 / 0.6
8	0.96 ± 0.13 0.08 / 0.003	0.75 ± 0.14 0.5 / 0.02	0.60 ± 0.17 0.6 / 0.1	0.60 ± 0.17 0.7 / 0.1
9	1.05 ± 0.15 0.4 / 0.04	0.75 ± 0.14 2 / 0.2	0.59 ± 0.21 3 / 1	0.59 ± 0.21 3 / 1
10	1.03 ± 0.14 0.04 / 0.004	0.73 ± 0.14 0.4 / 0.03	0.59 ± 0.21 0.5 / 0.3	0.59 ± 0.21 0.7 / 0.3

Table 3: Trend estimates for different periods and probability for occurrence in random data

1966-2005	1966-1985	1986-2005
Trend [$10^6\text{km}^3/\text{year}$] prob1 / prob2 [%]	Trend [$10^6\text{km}^3/\text{year}$] prob1 / prob2 [%]	Trend [$10^6\text{km}^3/\text{year}$] prob1 / prob2 [%]
0.99 ± 0.11 0.04 / <0.0001	1.11 ± 0.37 2.2 / 0.4	1.70 ± 0.34 3.5 / 0.2

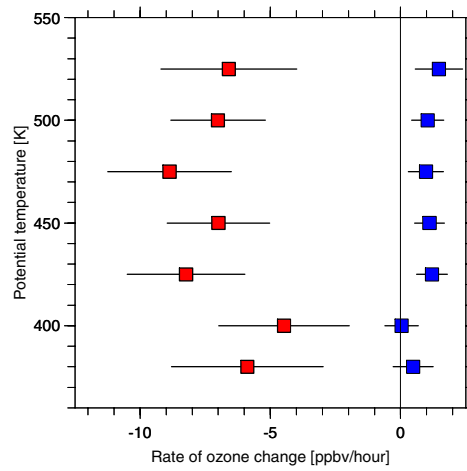


Figure 5. Ozone loss rate (ppbv/hr) between 5 Jan and 10 Feb 2005 versus Θ , where ozone loss rates are calculated separately for the sunlit and for the dark portions of the trajectories. Error bars denote 1σ statistical uncertainties.

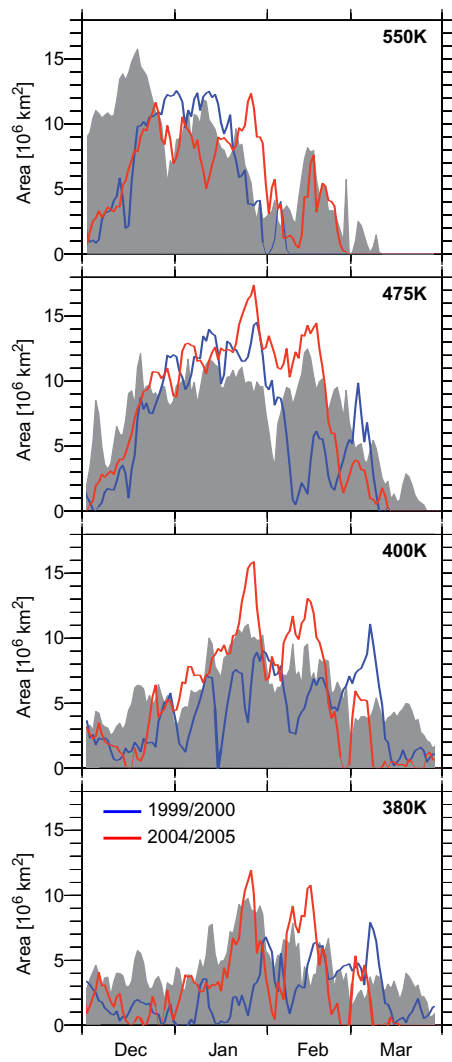


Figure 6. Time series of A_{PSC} for December to March of winter 2000 (blue) and 2005 (red) at the $\Theta = 380, 400, 475$ and 550 K levels. Gray shading indicates the range of A_{PSC} between 1992 and 2004 (excluding the winter of 2000). Here, A_{PSC} denotes the *daily* horizontal extent of temperatures low enough for PSCs to exist (in the main paper, we use A_{PSC} to refer to the average value of this quantity over winter).

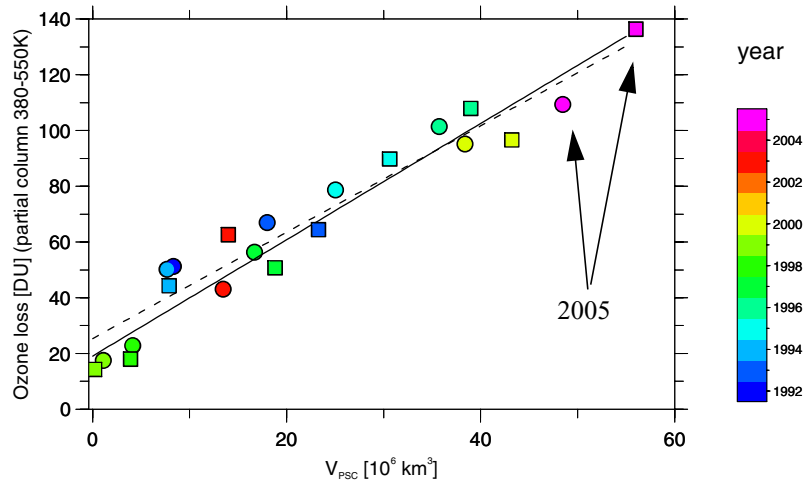


Figure 7. ΔO_3 versus V_{PSC} for various Arctic winters calculated for $e\theta$ between 400 and 550 K (circles, dashed fit line) and for $e\theta$ between 360 and 550 K (boxes, solid fit line). The 400 to 550 K points, for winters prior to 2005, are from *Rex et al.* [2004].